Radiology Case Reports 18 (2023) 4160–4166

Available online at www.sciencedirect.com

ScienceDirect

journal homepage: www.elsevier.com/locate/radcr

Case Report

A rare case of epithelial-myoepithelial carcinoma ex pleomorphic adenoma of the parotid gland: Radiologic-pathologic correlation ☆

Chika Yamada, MD[a,], Akira Baba, MD, PhD[a], Hideomi Yamauchi, MD, PhD[a], Nobuhiro Ogino, MD, PhD[a], Masato Nagaoka, MD[b], Ai Iwauchi, MD[c], Miku Maeda, MD[c], Nei Fukasawa, MD[c], Masayuki Shimoda, MD, PhD[c], Taisuke Mori, MD, PhD[d], Hiroya Ojiri, MD, PhD[a]*

[a] *Department of Radiology, The Jikei University School of Medicine, 3-25-8, Nishi-Shimbashi, Minato-ku, Tokyo, 1058461, Japan*
[b] *Department of Otorhinolaryngology, The Jikei University School of Medicine, Tokyo, Japan*
[c] *Department of Pathology, The Jikei University School of Medicine, Tokyo, Japan*
[d] *Department of Diagnostic Pathology, National Cancer Center Hospital, Tokyo, Japan*

ARTICLE INFO

Article history:
Received 9 June 2023
Revised 21 August 2023
Accepted 22 August 2023

Keywords:
Carcinoma ex pleomorphic adenoma
Epithelial-myoepithelial
Parotid gland
Case report
Radiologic-pathologic

ABSTRACT

Carcinoma ex pleomorphic adenoma is a carcinoma that arises from a primary or recurrent benign pleomorphic adenoma. The prevalence of epithelial-myoepithelial carcinoma is low, and this histological type accounting for only 1% of all salivary gland tumors. Here, we report a rare case of Epithelial-Myoepithelial Carcinoma ex pleomorphic adenoma of the parotid gland with a radiologic-pathologic correlation.

☆ Competing Interests: The authors declare that they have no known competing financial interests or personal relationships that could have appeared to influence the work reported in this paper.

* Corresponding author.
E-mail address: chika0412yamada@yahoo.co.jp (C. Yamada).

https://doi.org/10.1016/j.radcr.2023.08.099

Introduction

Carcinoma ex pleomorphic adenoma (CXPA) is a carcinoma that arises from a primary or recurrent benign pleomorphic adenoma [1]. The prevalence of CXPA is low, ranging from 2.4 to 6.3 in 100,000 malignant tumors [2]. The most common histological types are salivary duct carcinoma and myoepithelial carcinoma [3]. Epithelial myoepithelial carcinoma (EMCa) accounts for only 1% of all salivary gland tumors [4–6]. Here, we report a rare case of EMCa ex pleomorphic adenoma of the parotid gland with a radiologic-pathologic correlation.

Case presentation

A 61-year-old male presented to the otolaryngology clinic with an enlarged right-sided parotid mass. Twenty years ago, the patient noticed the mass and observed an increase in the size of his right parotid gland over the past 2 years with tenderness and pain. Fine-needle aspiration biopsy revealed malignancy, and the patient was referred to our hospital for surgery. The patient had no history of malignancies.

Physical examination revealed a solitary, well-defined, nodular mass in the right parotid gland measuring approximately 4 cm with poor mobility. The patient complained of pain while opening his mouth. However, no facial nerve deficits or cervical lymphadenopathy were observed. Tumor marker levels were within the normal range.

Magnetic resonance imaging (MRI) revealed a heterogeneous multinodular solid tumor measuring approximately 5 cm superficial to the deep right parotid gland, with partially irregular margins. The tumor covered the anatomical region of the main trunk of the facial nerve, although no perineural spread was observed. The tumor showed no extracapsular extension from the parotid gland. The T2-weighed image revealed a predominantly solid, ill-defined lesion with heterogeneous hyperintensity compared with the spinal cord (Figs. 1 and 2). There was a nodule measuring approximately 2 cm inside the tumor with a thick, low-intensity rim on the T2-weighed image (Figs. 1 and 2). The T1-weighed image revealed a homogeneous iso intensity lesion compared with the spinal cord (Fig. 3). Contrast-enhanced fat-suppressed T1-weighed image revealed an irregular, marginally dominant, heterogeneous, and moderately enhancing lesion (Figs. 4 and 5). Large and small focal, poorly enhanced areas were observed in the inner components of the tumor (Figs. 4 and 5). Diffusion-weighted imaging revealed a mildly hyperintense lesion (Fig. 6). The apparent diffusion coefficient (ADC) map showed a heterogeneous and relatively low ADC value. The mean ADC value was 1.106×10^{-3} mm^2/s. Additionally, a crescent lesion in the ventral and superior region with the highest ADC value of 1.522×10^{-3} mm, correlated with the ventral region of the largest poor enhancement area (Fig. 7). The smaller poor enhancement area, located in the ventral and deeper region, had an ADC value of 1.065×10^{-3} mm. The dorsal region of the tumor showed the lowest ADC value of 0.986×10^{-3} mm (Fig. 7). No cervical lymph node adenopathy was observed.

Computed tomography (CT) revealed marginal calcification around the nodule within the tumor (Fig. 8).

Considering these findings, we concluded that the patient had a malignant tumor of the right parotid gland and a carcinoma ex pleomorphic adenoma was suspected (radiologically T3N0M0 stage III).

Right radical parotidectomy with facial nerve sacrifice, right selective neck dissection (levels I-V), deep inferior epigastric perforator flap placement, left sural nerve reconstruction, and tracheostomy were performed.

Gross pathological imaging revealed that the right parotid gland measured 80 × 75 × 40 mm (Gross Pathology 1). The cut surface revealed a well-defined white tumor measuring 35 × 32 × 39 mm (Gross Pathology 2). The tumor infiltrated both the internal and external areas of the adjacent

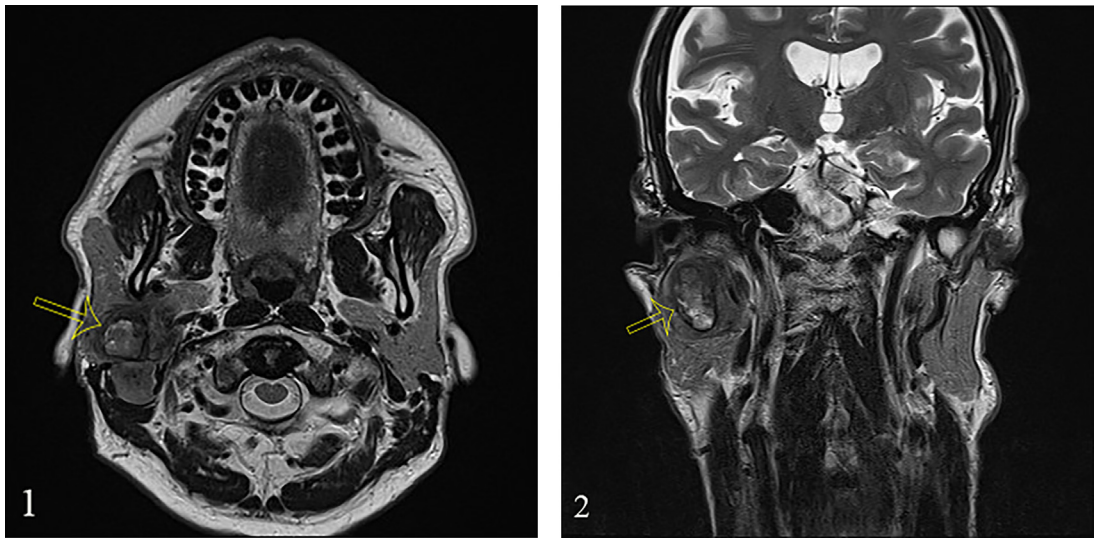

Figs. 1 and 2 – The T2-weighed axial (1) /coronal (2) images revealed a predominantly solid, ill-defined lesion with heterogeneous hyperintensity compared with the spinal cord. There was a nodule (arrow) measuring approximately 2 cm inside the tumor with a thick, low-intensity rim on the T2-weighed image.

Fig. 3 – The T1-weighed axial image revealed a homogeneous iso intensity lesion (asterisk) compared with the spinal cord.

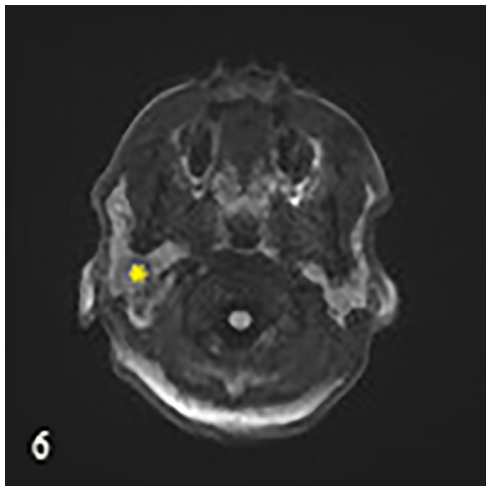

Fig. 6 – Diffusion-weighted imaging revealed a mildly hyperintense lesion (asterisk).

parenchyma and no fibrotic capsule was detected. Marginal invasion was positive and tumor infiltration of the digastric muscle tendon was observed. A well-defined yellow nodule was observed at the center of the tumor (Gross Pathology 2). Histopathology at lower magnification revealed a bundle of fiber tissue that formed a nodule (Histopathology 1). The ventral component of the nodule was an aggregated lesion of fiber tissue with edema and mucus retention. Invasion of atypical cells inside and outside the nodule was observed, and no apparent differences in cell and tissue structures were identified. No residual pleomorphic adenoma (PA) cells were observed inside the nodule. Necrotic areas were identified in the tumor. Partial perineural spread was observed; however, lymphovascular invasion was not detected. Histological findings at higher magnification revealed small nests and cord-like structures, and glandular cavities (epithelium) were occasionally observed (Histopathology 2). The tumor cells were mainly myoepithelial cells with a clear matrix and irregular swollen nuclei; however, the ductal structure was also partially recognized. In the stroma, prominent collagen fibers were accompanied by hyalinization. Immunohistochemistry revealed that the myoepithelium was positive for p63 and S100, and negative for αSMA and calponin. Ductal epithelium was positive for c-kit, EMA, and HER2. β-catenin was positive in the plasma membrane, and no AR expression was observed. Fur-

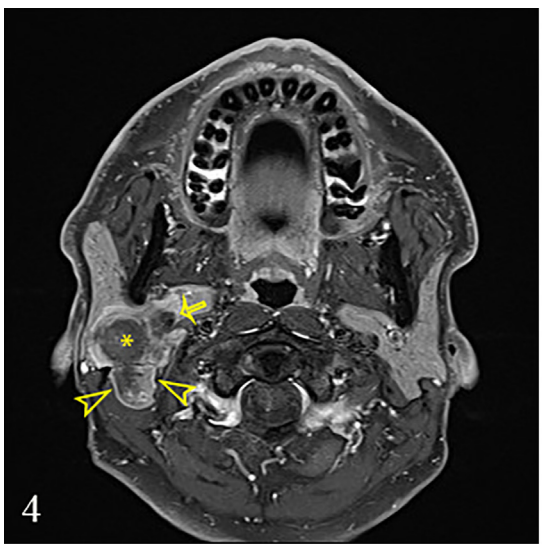

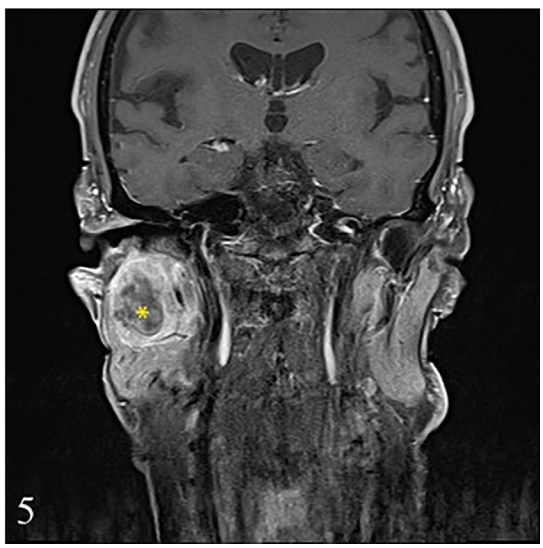

Figs. 4 and 5 – Contrast-enhanced fat-suppressed T1-weighed axial (4) /coronal (5) images revealed an irregular, marginally dominant, heterogeneous, and moderately enhancing lesion. Large (asterisk) and small (arrow and arrowhead) focal, poorly enhanced areas were observed in the inner components of the tumor.

Fig. 7 – The apparent diffusion coefficient (ADC) map showed a heterogeneous and relatively low ADC value. The mean ADC value was 1.106 x 10^{-3} mm^2/s. Additionally, a crescent lesion in the ventral and superior region (arrow) with the highest ADC value of 1.522 x 10^{-3} mm, correlated with the ventral region of the largest poor enhancement area. The dorsal region (circle) of the tumor showed the lowest ADC value of 0.986 x 10^{-3} mm.

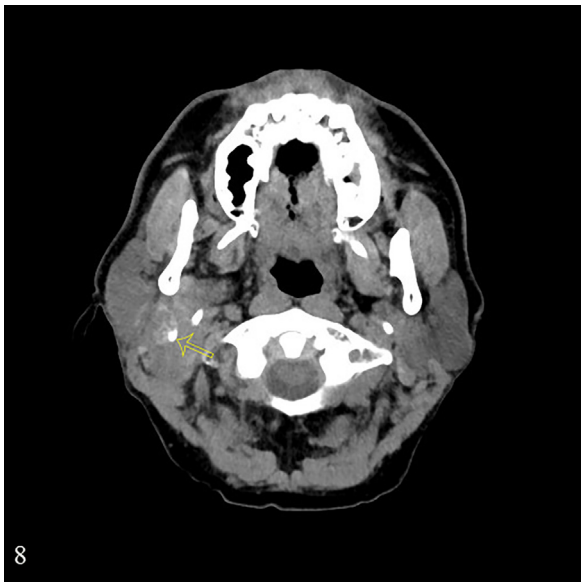

Fig. 8 – CT revealed marginal calcification around the nodule within the tumor (arrow).

thermore, the MIB-1 labeling index was approximately 20% (hotspot). Aggressive invasion of the surrounding tissues, tumor necrosis, perineural invasion, and high proliferative activity indicated a high-grade malignant tumor, suggesting that the most probable diagnosis was epithelial-myoepithelial carcinoma (EMCa) ex pleomorphic adenoma with no detected lymph node metastasis (pathological T3N0).

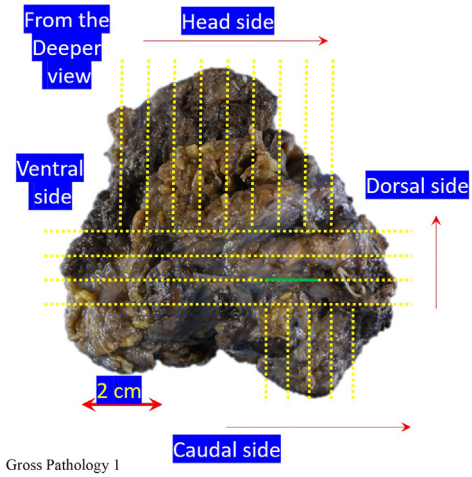

Gross Pathology 1 – Gross pathological imaging: Gross Pathology 1 and 2. Gross pathological imaging revealed that the right parotid gland measured 80 x 75 x 40 mm.

Histopathological examination revealed tumor infiltration around the styloid process and postoperative radiotherapy was scheduled. The patient received a total dose of 66 Gy/33 Fr. Approximately 1 year 5 months after surgery, no locoregional or metastatic recurrence was observed.

Discussion

Carcinoma ex pleomorphic adenoma (CXPA) is a carcinoma that arises from a primary or recurrent benign pleomorphic adenoma [1]. The prevalence of CXPA is low, ranging from 2.4 to 6.3 in 100,000 malignant tumors [2]. The most common histological types are salivary duct carcinoma and myoepithelial carcinoma [3]. EMCa accounts for only 1% of all salivary gland tumors, with an average age of onset of 60-70 years and slight female predominance [4–6]. Seethala et al. [7] encountered only 1 case of EMCa ex pleomorphic adenoma among 61 EMCa cases. Sedassari et al. [8] reported 3 new cases of EMCa ex-pleomorphic adenoma and found 9 further cases in their literature review. Therefore, EMCa rarely arises from preexisting PA [9,10]. Over 75% of EMCa develop in the parotid gland [11,12].

In typical CXPA cases, an MRI shows an ill-defined tumor accompanied by an intratumoral nodule with a thick, low-intensity rim on T2-weighed image [13]. This nodule within the tumor reflects preexisting PA, which pathologically reveals extensive hyalinization/fibrosis with myxoid stroma [14]. In our case, images revealed an ill-defined, heterogeneous hyperintense lesion compared with the spinal cord and a nodule with a thick low-intensity rim within the tumor on the T2-weighed image. These are typical CXPA imaging findings.

PA, salivary duct carcinoma, and high-grade mucoepidermoid carcinoma were included in the differential diagnosis based on the imaging findings. Lobulated, well-defined tu-

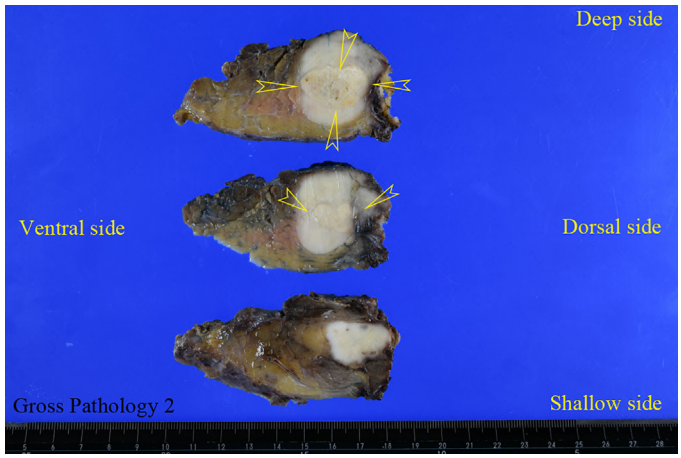

Gross Pathology 2 – The cut surface revealed a well-defined white tumor measuring 35 x 32 x 39 mm. A well-defined yellow nodule was observed at the center of the tumor (arrowhead).

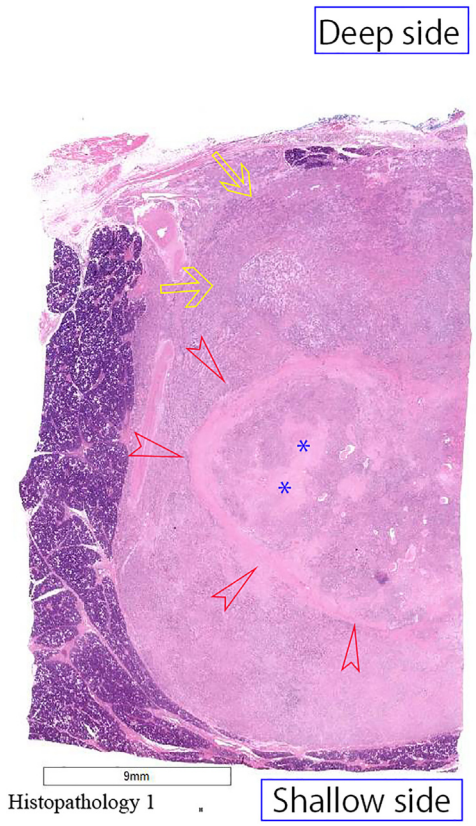

Histopathology 1 – Histopathology: Histopathology 1and2. Histopathology at lower magnification revealed a bundle of fiber tissue that formed a nodule (red arrowhead). The ventral component of the nodule was an aggregated lesion of fiber tissue with edema and mucus retention (blue asterisk). Invasion of atypical cells inside and outside the nodule was observed, and no apparent differences in cell and tissue structures were identified (yellow arrow).

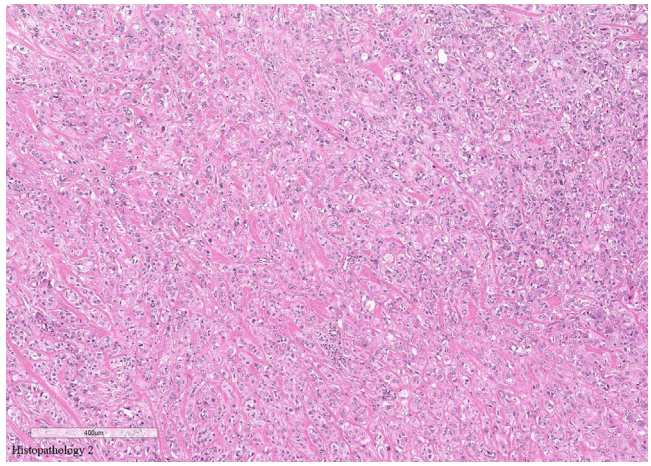

Histopathology 2 – Histological findings at higher magnification revealed small nests and cord-like structures, and glandular cavities (epithelium) were occasionally observed.

mors with high signal intensity on T2-weighed images, various enhancements after contrast administration, and relatively higher ADC values are well-known specific imaging findings of PA [15,16]. Salivary duct carcinoma and high-grade mucoepidermoid carcinoma are more likely to show low signal intensity on T2-weighed images to distinguish the present case from the affected cases [14].

Suto et al. [5] reviewed the MRI findings of EMCa of the parotid gland. In their study, imaging features were correlated with histopathological findings such as margin, capsule, multinodular structure, septa, predominance, and signal intensity patterns. They concluded that the parotid gland EMCa was predominantly a solid lesion with well-demarcated margins and capsules. Particularly, a multinodular structure with internal septa is a characteristic of EMCa. They also reported that local recurrence is common in EMCa, but an accurate preoperative diagnosis would lead to the selection of optimal treatment strategies to avoid overtreatment.

The present patient had a predominantly solid, ill-defined, multinodular lesion, which revealed heterogeneous hyperintensity on T2-weighed image and a heterogeneous moderately enhancing lesion after contrast administration without cap-

sule/internal septa. Most imaging features coincided with typical characteristics of EMCa, except for the absence of the capsule/internal septa. Additionally, our patient had a higher ADC than that reported in a previous study.

Considering the radiologic-pathologic correlation in this patient, we can refer to the following 3 findings:

First, our case revealed a typical imaging finding observed in CXPA; there was a nodule with a thick low-intensity rim on the T2-weighed image in the tumor. The nodule was surrounded by EMCa cells. The fact that no PA cells were present in the nodule is not necessarily sufficient to rule out CXPA as a differential diagnosis. Additionally, the characteristics of the cells inside and outside the nodule were similar, which was insufficient to rule out CXPA. We believe that pre-existing PA cells in the nodule are replaced by EMCa cells during malignant transformation.

Second, the thick, low-intensity rim of the intratumoral nodule on a T2-weighed image correlated with the bundle of fiber tissue, which is valid for the pseudocapsule of the pre-existing PA.

Third, the crescent lesion with the highest ADC value, which correlated with the ventral region of the largest poor enhancement area, pathologically corresponded to a congregated lesion of fiber tissue with edema and mucus retention.

Conclusion

In conclusion, although no PA cells were present in the nodule, the present patient showed typical CXPA imaging findings, and we considered that PA cells in the nodule were replaced by EMCa cells during malignant transformation. It is difficult to assume that the carcinomatous component type correlates with the imaging findings, especially in salivary gland tumors. The patient had some characteristic features on EMCa images and a relatively higher ADC value. Although the prevalence of EMCa is low, its ADC value is higher than that of salivary duct carcinoma. When encountering these imaging findings, the possibility of EMCa-ex PA should be considered.

Ethical considerations

Ethical approval was not necessary for the preparation of this article.

Patient consent

Written informed consent was obtained from the patient for publication of this case report and any accompanying images.

REFERENCES

[1] Antony J, Gopalan V, Smith RA, Lam AK. Carcinoma ex pleomorphic adenoma: a comprehensive review of clinical, pathological and molecular data. Head Neck Pathol 2012;6(1):1–9. doi:10.1007/s12105-011-0281-z.

[2] Gupta A, Koochakzadeh S, Neskey DM, Nguyen SA, Lentsch EJ. Carcinoma ex pleomorphic adenoma: a review of incidence, demographics, risk factors, and survival. Am J Otolaryngol 2019;40(6):102279. doi:10.1016/j.amjoto.2019.102279.

[3] Zhao J, Wang J, Yu C, Guo L, Wang K, Liang Z, et al. Prognostic factors affecting the clinical outcome of carcinoma ex pleomorphic adenoma in the major salivary gland. World J Surg Oncol 2013;8(1):180. doi:10.1186/1477-7819-11-180.

[4] Kusafuka K, Yamashita M, Muramatsu A, Arai K, Suzuki M. Epithelial-myoepithelial carcinoma ex-pleomorphic adenoma of the parotid gland: report of a rare case with immunohistochemical and genetic analyses. Med Mol Morphol 2021;54(2):173–80. doi:10.1007/s00795-020-00262-6.

[5] Suto T, Kato H, Kawaguchi M, Kobayashi K, Miyazaki T, Ando T, et al. MRI findings of epithelial-myoepithelial carcinoma of the parotid gland with radiologic-pathologic correlation. Jpn J Radiol 2022;40(6):578–85. doi:10.1007/s11604-021-01243-0.

[6] Suzuki M, Matsuzuka T, Saijo S, Takahara M, Harabuchi Y, Okuni T, et al. Carcinoma ex pleomorphic adenoma of the parotid gland: a multi-institutional retrospective analysis in the Northern Japan Head and Neck Cancer Society. Acta Otolaryngol 2016;136(11):1154–8. doi:10.1080/00016489.2016.1191671.

[7] Seethala RR, Barnes EL, Hunt JL. Epithelial-myoepithelial carcinoma: a review of the clinicopathologic spectrum and immunophenotypic characteristics in 61 tumors of the salivary glands and upper aerodigestive tract. Am J Surg Pathol 2007;31(1):44–57. doi:10.1097/01.pas.0000213314.74423.d8.

[8] Sedassari BT, Dos Santos HT, Mariano FV, da Silva Lascane NA, Altemani A, Sousa S. Carcinoma ex pleomorphic adenoma of minor salivary glands with major epithelial-myoepithelial component: clinicopathologic and immunohistochemical study of 3 cases. Ann Diagn Pathol 2015;19(3):164–8. doi:10.1016/j.anndiagpath.2015.03.011.

[9] Ahuja G, Taghipour DJ, Olufajo OA, Davis BC, Shokrani B, Bond WR Jr. A rare de novo myoepithelial carcinoma ex pleomorphic adenoma in a young woman. Case Rep Otolaryngol. 2020;26:8325374 2020. doi:10.1155/2020/8325374.

[10] Nandini DB, Singh WT, Aparnadevi P, Ningombam DS. Epithelial-myoepithelial carcinoma ex pleomorphic adenoma of the parotid gland with unique histologic differentiation: a rare case report. J Oral Maxillofac Pathol 2022;26(Suppl 1):S34–9. doi:10.4103/jomfp.jomfp_400_21.

[11] Vázquez A, Patel TD, D'Aguillo CM, Abdou RY, Farver W, Baredes S, et al. Epithelial-myoepithelial carcinoma of the salivary glands: an analysis of 246 cases. Otolaryngol Head Neck Surg 2015;153(4):569–74. doi:10.1177/0194599815594788.

[12] Wang F, Li B, Wang Y, Shen Y, Yang H. Clinical and pathological analysis of 10 cases of salivary gland epithelial-myoepithelial carcinoma. Medicine (Baltimore) 2020;9(41):e22671. doi:10.1097/MD.0000000000022671.

[13] Kashiwagi N, Murakami T, Chikugo T, Tomita Y, Kawano K, Nakanishi K, et al. Carcinoma ex pleomorphic adenoma of the parotid gland. Acta Radiol 2012;1(3):303–6 53. doi:10.1258/ar.2011.110389.

[14] Akutsu A, Horikoshi T, Yokota H, Wada T, Motoori K, Nasu K, et al. MR imaging findings of carcinoma ex pleomorphic adenoma related to extracapsular invasion and prognosis.

AJNR Am J Neuroradiol 2022;43(11):1639–45. doi:10.3174/ajnr.A7656.
[15] Kakimoto N, Gamoh S, Tamaki J, Kishino M, Murakami S, Furukawa S. CT and MR images of pleomorphic adenoma in major and minor salivary glands. Eur J Radiol 2009;69(3):464–72. doi:10.1016/j.ejrad.2007.11.021.
[16] Ikeda K, Katoh T, Ha-Kawa SK, Iwai H, Yamashita T, Tanaka Y. The usefulness of MR in establishing the diagnosis of parotid pleomorphic adenoma. AJNR Am J Neuroradiol 1996;17(3):555–9.